UNIVERSITÀ DEGLI STUDI DI PADOVA

DEPARTMENT OF MATHEMATICS “TULLIO LEVI-CIVITA”

# *Nematic Bubbles*

SILVIA PAPARINI
silvia.paparini@unipd.it

JOINT WORK WITH Gaetano Napoli[1]

01/04/2025

PISAN YOUNG SEMINARS IN APPLIED AND NUMERICAL MATHEMATICS

[1] Dipartimento di Matematica e Applicazioni Renato Caccioppoli, Università degli Studi di Napoli Federico II, Napoli, Italy.

# Nematic Liquid Crystals (LCs)

These systems flow like liquids while retaining an **orientational order**. This **local** alignment is described by a macroscopic unit vector field, the **director field** $\boldsymbol{n}$.

Their **degree** of orientation is represented by the **scalar order parameter** $q \in [0, 1]$.

- **Head-tail symmetry**: $\boldsymbol{n} \leftrightarrow -\boldsymbol{n}$.
- **Spatial distortions** of $\boldsymbol{n}$ are measured by $\nabla\boldsymbol{n}$. It becomes singular at **topological defects**.
- **Ground state** of nematics: uniform director field ($\nabla\boldsymbol{n} = \boldsymbol{0}$).
- $q = 0$ when the material is **isotropic** (no preferred orientation exists).

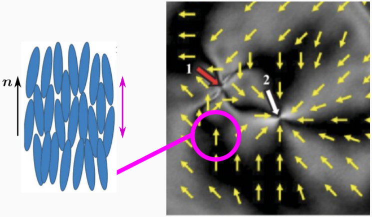


**rod-like** molecules: $5$ Å by $20$ Å.

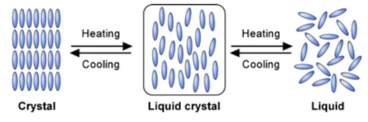


$q = 1$ $\quad$ $q \in (0, 1)$ $\quad$ $q = 0$

The nematic phase can be induced in a mesogenic substance by changing its temperature.
This corresponds to a change in $q$.

# Thin Nematic Shells

Thin layers of nematic liquid crystal confined to a closed, curved surface.

The geometry induces a distortion in the molecular orientation and, for sufficiently thin shells, forces the director field $\boldsymbol{n}$ to lie **tangent** to the surface (e.g., $\boldsymbol{n}$ coating a spherical colloidal droplet with radius $R \sim 50\,\mu\mathrm{m}$ and thickness $\sim 1\,\mu\mathrm{m}$)

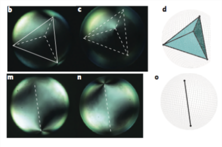

T. Lopez-Leon et al, Nature Physics, 2011

**Hairy ball theorem**:

there is **no** nonvanishing **continuous tangent vector field** on a sphere.

**Unavoidable** defects arise when nematic order is established on a surface with a spherical topology.

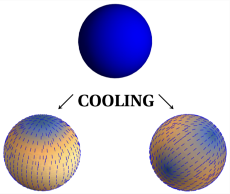

Defects in $\boldsymbol{n}$ are classified by their **topological charge** $m$, defined as the **winding number** of $\boldsymbol{n}$ on the tangent plane of the defect.

## Example of topological charge in the plane

$$\boldsymbol{n} = \cos w \boldsymbol{e}_r + \sin w \boldsymbol{e}_\vartheta, \quad w = w(\vartheta) = (m-1)\vartheta + \vartheta_0$$

$(\boldsymbol{e}_r, \boldsymbol{e}_\vartheta, \boldsymbol{e}_z)$ standard cylindrical frame, $\vartheta_0$: phase

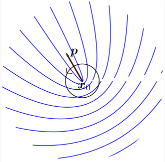


$q = +\frac{1}{2},\ \vartheta_0 = \frac{\pi}{3}$

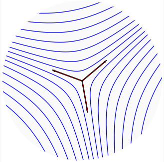

$q = -\frac{1}{2},\ \vartheta_0 = \frac{\pi}{3}$

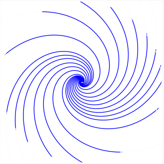

$q = +1,\ \vartheta_0 = \frac{\pi}{3}$

**By the Poincaré-Hopf theorem**: Any tangent vector field on a sphere, or any surface topologically equivalent to it, must have a total topological charge equal to $+2$.

# Topological Defects in Hydra Morphogenesis

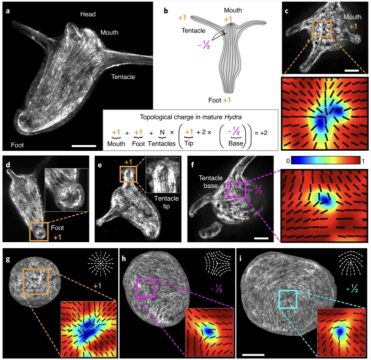


In Hydra ectoderm, actin fibers form a nematic phase.

Topological defects in the nematic order acts as **organizing centers in morphogenesis**, enabling organism to grow protrusions or deplete material to **relive stress**.

- $+1$ **defects**: **Stable** organizers located at the head (mouth), foot, and tentacle tips.
- $+1/2$ **defects**: Transient, **mobile** structures during early regeneration. They migrate and merge at specific sites (often the foot) to form stable $+1$ organizers.
- $-1/2$ **defects**: Localized at **saddle-shaped regions**, namely the tentacle bases, to perfectly balance the $+1$ charge of the tips.

# Stantard Uniaxial Regeneration

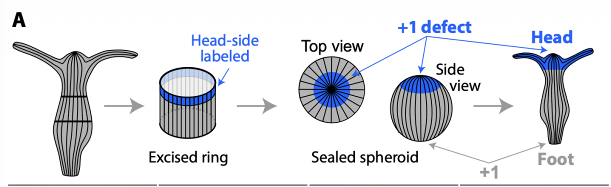


Early stages following the excision of a fragment of *Hydra*:

1. **Excision and Folding**: The inherited nematic arrangement of actin fibres is lost within hours as the tissue folds into a **closed spheroid**.
2. **Induction of Order**: Actin fibres realign, but the closed geometry imposes **topological constraints**, necessarily generating defects.
3. **Structural Memory**: This induction of order confers a structural memory of the original **body axis orientation** at the earliest regeneration stages.
4. **Emergence of Morphological Features**: Two $+1$ defects emerge at the forming mouth and foot. The apical defect dictates **tissue rupture** (mouth formation), while the basal region remains closed.

# Nematic Bubbles

*To investigate the molecular origin of muscle fibre alignment and its interplay with the mechanics of a deformable surface during Hydra regeneration . . .*

**Biological System**

Excised tissue folding into a **closed spheroid**, with consequent **induction of order** into the nematic fibers.

$\Longleftrightarrow$

**Mathematical model: Nematic Bubble**

Deformable surface coated with a nematic liquid crystal tangent to the surface

**Modelling the Mechanism:**

$$\text{Isotropic shell} \xrightarrow{\textbf{Cooling}} \text{Nematic ordering} \xrightarrow{\textbf{Symmetry breaking}} \text{Shape deformation.}$$

*Cooling mimics the natural induction of nematic order in the muscle fibres.*

# Model and energy landscape

We model the nematic bubble as a regular closed surface $S$ (*topologically equivalent to a sphere*), equipped with an outward unit normal $\boldsymbol{\nu}$.

$$W[S] = \underbrace{\gamma\,\mathrm{area}(S) - \mu(\mathrm{vol}(S) - V_0)}_{\text{Classical soap bubble}} + \underbrace{\int_S \rho w_n \, dA}_{\text{Nematic Contribution}}$$

$\gamma > 0$: surface tension, $V_0$: fixed enclosed volume,

$\mu$: Lagrange multiplier *(associated with the volume constraint)*

$\rho$: mass density, $w_n$: nematic distortion energy density *(per unit mass)*

**Classical Soap Bubble**: Equilibrium is governed by the **Young-Laplace law**.

This law balances the **pressure difference** $\mu = \mathrm{P}_{\mathrm{in}} - \mathrm{P}_{\mathrm{out}}$ and surface tension $\gamma$ for a spherical bubble of radius $r_0$.

$$\boxed{\mu = \frac{2\gamma}{r_0}}$$

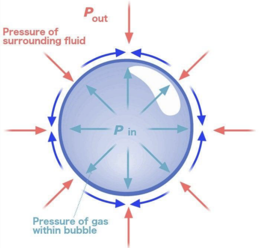

# Nematic contribution

$$\boxed{w_{\mathrm{n}} = w_{\mathrm{nem}} + w_{LdG}}$$

**Lexicon:**

G.N. and L. Vergori, Phys. Rev. E 85,061701 (2012)

$\nabla_s q = \mathbf{P}\nabla q, \quad \nabla_s \boldsymbol{n} = (\nabla \boldsymbol{n})\mathbf{P},$ (surface gradients)

$\mathbf{P} = \mathbf{I} - \boldsymbol{\nu} \otimes \boldsymbol{\nu}$ (orthogonal projector over the local tangent plane)

$\nabla$ (3D gradient of the extended field)

$\mathbf{L} = -\nabla_s \boldsymbol{\nu}$ (extrinsic curvature tensor).

## Nematic distortion energy density

$$w_{\mathrm{nem}} = \frac{k}{2}\left[\underbrace{\frac{1}{2}|\nabla_s q|^2 + 2q^2|\nabla_s \mathbf{n}|^2}_{(\mathbf{1})} - 2q^2 \underbrace{|\mathbf{Ln}|^2}_{(\mathbf{2})} + 2q \underbrace{\left(|\mathbf{Ln}|^2 - \frac{1}{2}\mathrm{tr}(\mathbf{L}^2)\right)}_{(\mathbf{3})} + \frac{(q^2+1)}{2}\underbrace{|\mathbf{L}|^2}_{(\mathbf{4})}\right]$$

**(1)** energetic cost associated to non-uniform states.

**(2)** favors the alignment of $\boldsymbol{n}$ with the principal directions of surface curvature.

**(3)** $= 2H\varsigma$ where $H$ is the mean curvature, and $\varsigma$ is the asphericity.

**(4)** Form of curvature elasticity imparted to the surface by $\boldsymbol{n}$, arising from the constraint that the field must remain tangent.

*Note:* **(4)** does not vanish even when the nematic is in the isotropic phase.

## Landau-de Gennes energy density

$$w_{\mathrm{LdG}} = \frac{a}{2}q^2 + \frac{c}{4}q^4 \tag{1}$$

$$a = a_0 \frac{T - T_{\mathrm{NI}}}{T_{\mathrm{NI}}} \quad (a_0, c > 0 \text{ constants})$$

$T_{\mathrm{NI}}$: Nematic-isotropic transition temperature

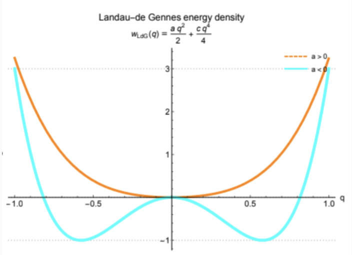


**Isotropic Phase**

$(T \geq T_{\mathrm{NI}} \implies a \geq 0)$

Single convex well
Minimum at $q = 0$
Isotropic state

---

**Nematic Phase**

$(T < T_{\mathrm{NI}} \implies a < 0)$

**Double well** potential
Minima at $q_{\mathrm{eq}} = \pm\sqrt{-a/c}$
Emergence of nematic order.

**Equilibrium Equations**: $\delta W = 0$.

Euler–Lagrange equations associated with $W$, obtained by considering **mass-preserving variations** and allowing **only virtual displacements orthogonal to the shell surface**.

**Transport theorem:** $\delta \int_{\mathcal{S}} \rho\, w_{\rm n}\, da = \int_{\mathcal{S}} \rho\, \delta w_{\rm n}\, da$

---

**Euler Lagrange equations:**

$$-2\gamma H - \mu + \mathrm{div}_s(\mathbf{P}\,\mathrm{div}_s\boldsymbol{\Lambda} + \boldsymbol{\nu}\cdot\mathrm{div}_s\mathbf{G}\,\mathbf{n}) + \boldsymbol{\Lambda}\cdot\mathbf{L}^2 + \mathbf{G}\cdot(\nabla_s\mathbf{n})\mathbf{L} + \boldsymbol{\zeta}\cdot\mathbf{L}\nabla_s q = 0 \qquad \boxed{\text{shape eqn}},$$

$$\mathbf{t}\cdot(\mathbf{g} - \mathrm{div}_s\mathbf{G}) = 0 \qquad \boxed{\boldsymbol{n}\text{ eqn}},$$

$$\xi - \mathrm{div}_s\boldsymbol{\zeta} = 0 \qquad \boxed{q\text{ eqn}}$$

where

$$\boldsymbol{\Lambda} = \frac{k\rho}{2}\left[2q(1-q)(\mathbf{L}\mathbf{n}\otimes\mathbf{n} + \mathbf{n}\otimes\mathbf{L}\mathbf{n}) + (q^2 - 2q + 1)\mathbf{L}\right]$$

$$\mathbf{G} = 2\rho k q^2\nabla_s\mathbf{n}, \qquad \mathbf{g} = 2\rho k q(1-q)\mathbf{L}^2\mathbf{n}, \qquad \boldsymbol{\zeta} = \frac{k\rho}{2}\nabla_s q,$$

$$\xi = \rho\left[aq + cq^3 + \frac{k}{2}(2|\mathbf{L}\mathbf{n}|^2 - \mathbf{P}\cdot\mathbf{L}^2 + q(4|\nabla_s\mathbf{n}|^2 - 4|\mathbf{L}\mathbf{n}|^2 + |\mathbf{L}|^2))\right]$$

## Ground State solution: isotropic tangent plane $(q = 0)$

The $\boxed{q \text{ eqn.}}$ gives the **equilibrium condition**:

$$H\varsigma = 0 \quad \begin{array}{l} \nearrow \quad H = 0 \quad \text{(Minimal surfaces)} \\ \searrow \quad \boxed{\varsigma = 0 \quad \textbf{Isotropic Spherical Shell}} \end{array}$$

($H$: mean curvature, $\varsigma$: asphericity)

$$\Downarrow$$

*The* $\boxed{\textit{shape eqn}}$ *reduces to the* **Modified Young-Laplace law:**

$$\mu = \frac{2}{r_0}\left(\gamma \boxed{-\frac{k\rho_0}{2r_0^2}}\right) \tag{4}$$

radius $r_0 = \sqrt{\frac{3V_0}{4\pi}}$ constant mass density $\rho = \rho_0$

The additional term $\boxed{\cdot}$ arises from the curvature elasticity

# Linearization about the ground state

$(\boldsymbol{e}_r, \boldsymbol{e}_\vartheta, \boldsymbol{e}_\varphi)$ spherical frame.

$$\mathbf{p} = r(\vartheta, \varphi)\, \boldsymbol{e}_r \ \in \mathcal{S} \qquad \text{(non-axisymmetric bubble shapes)}$$

$$\boldsymbol{n} = \sin\alpha\, \mathbf{e}_1 + \cos\alpha\, \mathbf{e}_1^\perp, \qquad \alpha = \alpha(\vartheta, \varphi) \tag{5a}$$

$(\mathbf{e}_1, \mathbf{e}_1^\perp)$: local orthonormal basis on the tangent plane to $\mathcal{S}$

## Bifurcation from the trivial solution $(q = 0,\, r = r_0)$:

The **onset** of nematic ordering is modelled by the Landau-de Gennes parameter $a$ decreasing below a critical threshold $a_{\rm cr} < 0$.

***First-order expansion:*** We study solutions close to the isotropic sphere by introducing a small dimensionless parameter $\varepsilon \ll 1$:

$$q(\vartheta, \varphi) = \varepsilon q_1(\vartheta, \varphi), \qquad r(\vartheta, \varphi) = r_0 + \varepsilon r_1(\vartheta, \varphi) \tag{6}$$

$\varepsilon$: measures small departures of $a$ from its critical value $a_{\rm cr}$.

## The Linearised Eigenvalue Problem

Complex variable: $\mathcal{Q}_1 = q_1 \mathrm{e}^{2\mathrm{i}\alpha}$

$$\left.\begin{aligned} \eth_\sigma &= \partial_\vartheta - \mathrm{i}\csc\vartheta\,\partial_\varphi - \sigma\cot\vartheta \\ \bar{\eth}_\sigma &= \partial_\vartheta + \mathrm{i}\csc\vartheta\,\partial_\varphi + \sigma\cot\vartheta \end{aligned}\right\}$$ spin-raising/lowering operators

$\boxed{q \text{ eqn.}}$ and $\boxed{\boldsymbol{n} \text{ eqn.}}$ $\Rightarrow$ $$\frac{k}{r_0^2}\eth_1(\bar{\eth}_2\mathcal{Q}_1) - a\mathcal{Q}_1 - 2\frac{k}{r_0^3}\eth_1(\eth_0 r_1) = 0$$

$\boxed{\text{Shape eqn.}}$ $\Rightarrow$ $$\left[-\gamma + k\rho_0\left(\Delta_s^0 + \frac{5}{r_0^2}\right)\right]\left(\Delta_s^0 + \frac{2}{r_0^2}\right) r_1 + 2\frac{k\rho_0}{r_0^3}\mathrm{Re}[\bar{\eth}_1(\bar{\eth}_2\mathcal{Q}_1)] = 0$$

$\boxed{\text{Volume pres.}}$ $\Rightarrow$ $$\int_0^{2\pi}\int_0^{\pi} r_1(\vartheta,\varphi)\sin\vartheta\;\mathrm{d}\vartheta\;\mathrm{d}\varphi = 0$$

Laplace-Beltrami operator: $$\Delta_s^0 = \frac{1}{r_0^2}\left[\csc\vartheta\,\partial_\vartheta(\sin\vartheta\,\partial_\vartheta) + \csc^2\vartheta\,\partial_{\varphi\varphi}\right]$$

# Linear Analysis

We expand the unknowns in terms of **classical spherical harmonics** $Y_{lm}(\vartheta,\varphi)$ and **spin-weighted spherical harmonics of spin weight 2**, ${}_2Y_{lm}(\vartheta,\varphi)$:

$$\mathcal{Q}_1(\vartheta,\varphi)=\sum_{l=1}^{\infty}\sum_{m=-l}^{l} Q_{lm}\,{}_2Y_{lm}(\vartheta,\varphi),\qquad r_1(\vartheta,\varphi)=\sum_{l=1}^{\infty}\sum_{m=-l}^{l} R_{lm}\,Y_{lm}(\vartheta,\varphi) \quad (8)$$

$Q_{lm}, R_{lm}$: complex expansion coefficients.

The system of linear PDEs transforms into a homogeneous linear system for the variables $(Q_{lm}, R_{lm})$:

$$\begin{pmatrix} \dfrac{k\rho_0(l^2+l-2)}{r_0^2}+a\rho_0 & \dfrac{2k\rho_0\sqrt{l(l+1)(l^2+l-2)}}{r_0^3} \\ \dfrac{2k\rho_0\sqrt{l(l+1)(l^2+l-2)}}{r_0^3} & -\dfrac{(l^2+l-2)}{r_0^2}\left(-\gamma+\dfrac{k\rho_0\,(5-l(l+1))}{r_0^2}\right) \end{pmatrix}\begin{pmatrix} Q_{lm} \\ R_{lm}\end{pmatrix}=\begin{pmatrix}0\\0\end{pmatrix}$$

**Reality condition:** $Q_{lm}=(-1)^m Q^*_{l,-m}$

Non-trivial solutions exist provided the determinant vanishes, yielding the **eigenvalues**:

$$a_l=-\frac{k(l^2+l-2)}{r_0^2}-\frac{4k^2\rho_0\,l(l+1)}{r_0^4\left(-\gamma+\dfrac{k\rho_0(5-l(l+1))}{r_0^2}\right)} \qquad l\geq 2 \quad (9)$$

Note: For each $l$, there are $2l+1$ degenerate modes.

# Eigenvalues and Bifurcation Threshold

**Critical Threshold ($l = 2$):** The onset of nematic ordering occurs at the maximum eigenvalue within the spectrum:

$$a_{\mathrm{cr}} := a_2 = -\frac{2k}{r_0^2} + \frac{24k^2\rho_0}{r_0^4\left(\gamma + \frac{k\rho_0}{2r_0^2}\right)} \tag{10}$$

Solving the linear system for this mode yields the amplitude ratio:

$$\Lambda_{\mathrm{cr}} := \frac{Q_{2m}}{R_{2m}} = -\frac{1}{\sqrt{6}}\left(\frac{2\gamma r_0}{k\rho_0} + \frac{1}{r_0}\right) \tag{11}$$

| $m$ | $\Lambda_{\mathrm{cr}} \cdot r_1$ **eigenfunctions** | $\mathcal{Q}_1$ **eigenfunctions** |
|---|---|---|
| $-2, 2$ | $\sqrt{\frac{15}{8\pi}} \sin^2\vartheta \; (\mathrm{Re}[Q_{22}]\cos 2\varphi - \mathrm{Im}[Q_{22}]\sin 2\varphi)$ | $\frac{1}{2}\sqrt{\frac{5}{\pi}}\left(Q_{22}\mathrm{e}^{2\mathrm{i}\varphi}\cos^4\frac{\vartheta}{2} + Q_{22}^*\mathrm{e}^{-2\mathrm{i}\varphi}\sin^4\frac{\vartheta}{2}\right)$ |
| $-1, 1$ | $\sqrt{\frac{15}{8\pi}} \sin 2\vartheta \,(-\mathrm{Re}[Q_{21}]\cos\varphi + \mathrm{Im}[Q_{21}]\sin\varphi)$ | $\sqrt{\frac{5}{\pi}}\sin\frac{\vartheta}{2}\cos\frac{\vartheta}{2}\left(Q_{21}\mathrm{e}^{\mathrm{i}\varphi}\cos^2\frac{\vartheta}{2} - Q_{21}^*\mathrm{e}^{-\mathrm{i}\varphi}\sin^2\frac{\vartheta}{2}\right)$ |
| $0$ | $\frac{1}{4}\sqrt{\frac{5}{\pi}}\mathrm{Re}[Q_{20}](3\cos^2\vartheta - 1)$ | $\frac{1}{4}\sqrt{\frac{15}{2\pi}}\mathrm{Re}[Q_{20}]\sin^2\vartheta$ |

**Equivalences:**

A change in the phase of the complex coefficients simply results in a rigid transformation of the solutions.

Modes $(-2, 2)$ and $(-1, 1)$ are equivalent: they differ by a rigid transformation.

We employ a **weakly non-linear** analysis to both characterize the type of the bifurcation and the mode amplitudes.

# $m = 0$ Axisymmetric mode

Two $+1$ point defects situated at the poles.

## Prolate Shape

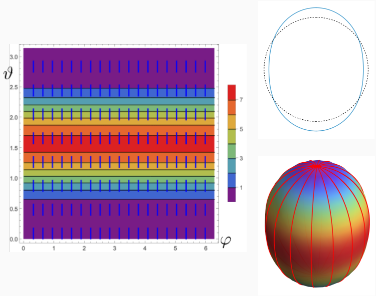


Director aligns along **meridians**

## Oblate Shape

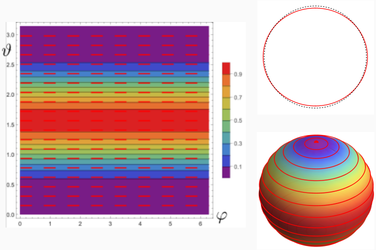


Director aligns along **parallels**

Darkest regions indicate the topological defects.

## $m = -1,\, 1$ $\quad m = -2,\, 2$ **Squared (non-axisymmetric) Modes**

**four $+\frac{1}{2}$ defects located at the vertices of a square**

**Mode $m = 1,\, -1$**

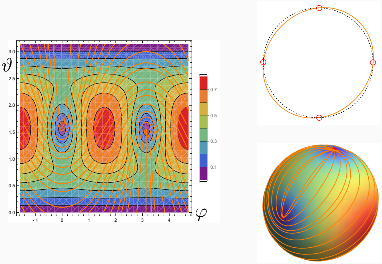


**Mode $m = -2,\, 2$**

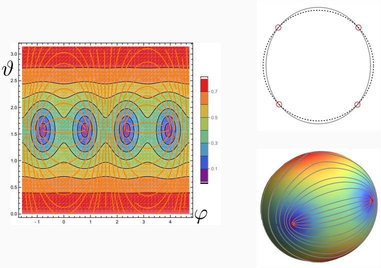


**2 defects** at poles
**2 defects** on equator ($\vartheta = \pi/2$)

All **4 defects** lie on the equator

Modes $m = -1,\, 1$ and $m = -2,\, 2$ represent the **same physical configuration**. They can be mapped onto each other via a rigid transformation.

# Energy Landscapes and Bifurcation Analysis

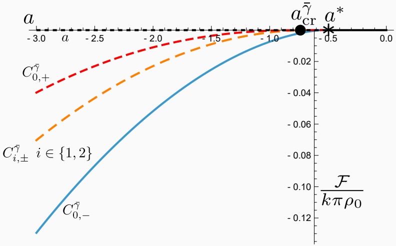


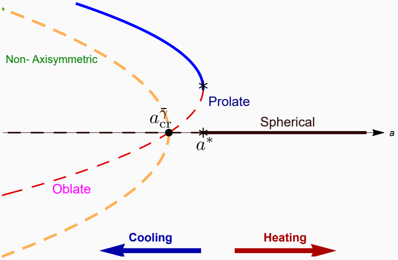


### Emergence of Bifurcated Modes:

- $a > a^\star$: Only the isotropic ground-state exists.
- $a = a^\star$: Axisymmetric modes emerge via a *discontinuous* bifurcation.
- $a < a^\star$: Trivial state coexists with prolate and oblate solutions.
- $a = a_{\rm cr}^{\bar\gamma}$: Non-axisymmetric modes arise via a *continuous* bifurcation.
- $a < a_{\rm cr}^{\bar\gamma}$: All bifurcated modes coexist at equilibrium.

Upon cooling, the system can undergo an abrupt transition from the isotropic to the **stable** prolate state.

Remaining non-trivial branches represent experimentally observable local minima.

# Bifurcation-Induced Mass Redistribution

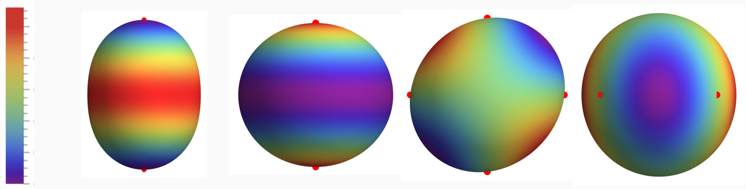

Color maps illustrate $\rho$ for the bifurcated configurations:
**Red:** local increase of $\rho$ (shell thickening), **Violet:** local decrease of $\rho$ (shell thinning),
**Green:** $\rho = \rho_0$ (no local mass redistribution).

**Topological Defects Signature:**

- **Integer $(+1)$ defects:** Induce significant local mass variations in axisymmetric shapes $(m = 0)$:

  *Prolate (a):* Thinning at the poles, thickening at the equator.
  *Oblate (b):* Thickening at the poles, thinning at the bulging equator.

- **Half-integer $(+1/2)$ defects** in non-axisymmetric modes $m = -1,\, 1$ and $m = -2,\, 2$:

  $\hookrightarrow$ **No mass variation** (green) occurs at their exact locations.

# Conclusions and Future Perspectives

G. Napoli and S. Paparini, *Nematic Bubbles and the Breaking of Spherical Symmetry*, arXiv:2603.07082 (2026).

Our findings can provide a mathematical framework for understanding defect-mediated morphogenesis in biological systems.

- **Mechanical Body Axis:** The globally stable prolate shape naturally establishes a **pole-to-pole axis**. This provide a purely mechanical pathway for establishing a body axis.
- **Defect-Mass Coupling:** Integer $(+1)$ defects act as primary organizing centres, driving significant local mass/thickness variations. Conversely, half-integer $(+1/2)$ defects do not perturb the local mass density in their immediate vicinity.

**Future Directions:**

- **Numerical Benchmark:** The analytical solutions derived can provide a benchmark for the validation of future numerical codes, particularly near the critical bifurcation threshold.
- **Negative Topological Defects:** Exploring higher-order eigenvalues to capture the $-1/2$ defects observed at the base of emerging *Hydra* tentacles.
- **Active Mechanics:** Future extensions of this model incorporating active stresses and dynamic fluid flows to capture the continuous energy consumption and out-of-equilibrium dynamics inherent to living tissues.